A New Method for Joint Susceptibility Artefact Correction and Super-Resolution for dMRI

Lars Ruthotto[a], Siawoosh Mohammadi[b], Nikolaus Weiskopf[b]

[a] University of British Columbia, Vancouver, Canada;
[b]Wellcome Trust Centre for Neuroimaging, University College London, United Kingdom;

ABSTRACT

Diffusion magnetic resonance imaging (dMRI) has become increasingly relevant in clinical research and neuroscience. It is commonly carried out using the ultra-fast MRI acquisition technique Echo-Planar Imaging (EPI). While offering crucial reduction of acquisition times, two limitations of EPI are distortions due to varying magnetic susceptibilities of the object being imaged and its limited spatial resolution. In the recent years progress has been made both for susceptibility artefact correction and increasing of spatial resolution using image processing and reconstruction methods. However, so far, the interplay between both problems has not been studied and super-resolution techniques could only be applied along one axis, the slice-select direction, limiting the potential gain in spatial resolution. In this work we describe a new method for joint susceptibility artefact correction and super-resolution in EPI-MRI that can be used to increase resolution in all three spatial dimensions and in particular increase in-plane resolutions. The key idea is to reconstruct a distortion-free, high-resolution image from a number of low-resolution EPI data that are deformed in different directions. Numerical results on dMRI data of a human brain indicate that this technique has the potential to provide for the first time in-vivo dMRI at mesoscopic spatial resolution (i.e. 500 μm); a spatial resolution that could bridge the gap between white-matter information from ex-vivo histology (≈ 1 μm) and in-vivo dMRI (≈ 2000 μm).

Keywords: Super-resolution, Susceptibility artefact correction, Image Registration, Diffusion MRI

1. INTRODUCTION

Diffusion magnetic resonance imaging (dMRI) is a powerful technique that provides important biomarkers for clinical diagnoses and neurological research.[1] dMRI is based on diffusion-weighted images that are made sensitive to the microscopic movement of water molecules as they diffuse through tissue along different directions. The diffusion-sensitization, however, makes the images also extremely sensitive to any other form of movement that may be present such as subject motion. To reduce motion-sensitivity in dMRI, Echo-Planar Imaging (EPI), an ultra-fast MRI technique,[2] is mostly used.

While offering crucial reduction of acquisition times, a well-known drawback of EPI is its high sensitivity to local perturbations of the magnetic field that are largely present in the living human brain.[3] In particular, strong magnetic field perturbations can be caused by changes in the magnetic susceptibility at the interface of two materials with different magnetic properties. Consequently, EPI data suffers from nonlinear geometrical deformations and intensity modulations commonly referred to as *susceptibility artefacts*. Susceptibility artefacts complicate a voxel-by-voxel combination of diffusion information, obtained using EPI, with anatomical, images that are unaffected by distortion. Over recent years, many susceptibility artefact correction techniques evolved; see[4] and references therein. A particular class of correction techniques are *reversed gradient approaches*.[5] Noting that, in EPI, displacements are most prominent along the phase-encoding direction the idea is to estimate the field inhomogeneity based on two datasets acquired with reversed phase-encoding direction that show opposite distortion patterns. Subsequently, both images are corrected using automatic post-processing tools like HySCO.[6] Although distortions can be reduced considerably, using reverse gradient approaches in general yields *two* approximately, but not identical, corrected images from which the user may pick one or average both to improve the signal-to-noise ratio.

A second crucial limitation of dMRI is its spatial resolution. On clinical scanners, resolutions above $(2\text{mm})^3$ are standard while the thickness of white matter compartments (e.g. axons) are in the range of micro meters. Even using improved scanning hardware (e.g. Heinemann et al.[7] at 7T) spatial resolution is limited to about 1000 μm, making super-resolution techniques not only a cheap alternative but even mandatory for meso-scale, in-vivo

Medical Imaging 2014: Image Processing, edited by Sebastien Ourselin, Martin A. Styner, Proc. of SPIE Vol. 9034, 90340P · © 2014 SPIE
CCC code: 1605-7422/14/$18 · doi: 10.1117/12.2043591

dMRI. The basic idea of super-resolution techniques is to reconstruct one high-resolution image from multiple shifted, low-resolution images.[8] Recently, there were promising super-resolution schemes in dMRI that are based on sub-voxel shifts in slice-selection direction which is not Fourier encoded.[9–11] Due to the translational invariance of the Fourier transform, simple shifts of the whole object cannot be used to increase the in-plane resolution in slice-wise MRI acquisitions.[12] Consequently, a common drawback of current super-resolution approaches is that they are effective in one direction only and that susceptibility artefacts are neglected, limiting their potentials for increasing spatial resolution above 1000 μm.

This paper describes a new method for joint susceptibility artefact correction and increasing in-plane resolution in EPI-MRI. Our method *uses* susceptibility related distortions in a number of low-resolution EPI data obtained with different phase-encoding directions to reconstruct *one* distortion free image with higher resolution. Because our approach uses nonlinear deformations, the argument of[12] against Fourier-encoded super-resolution does not apply. Results on dMRI data of a human brain indicate the potential of the proposed method to provide for the first time in-vivo dMRI at mesoscopic spatial resolution (i.e. 500 μm); a spatial resolution that could bridge the gap between white-matter information from histology (≈ 1 μm) and dMRI (≈ 2000 μm).

2. METHODS

The relation between a distorted EPI acquisition $\mathcal{I}^{\mathrm{EPI}}$ and the accurate image $\mathcal{I}$ by a physical distortion model has been established in.[5] Assuming continuos images and a known field inhomogeneity $\mathcal{B} : \Omega \to \mathbb{R}$, where $\Omega \subset \mathbb{R}^3$ is a domain, both images satisfy

$$\mathcal{I}(x) = \mathcal{I}^{\mathrm{EPI}}(x + \mathcal{B}(x)v)\,(1 + \partial_v \mathcal{B}(x)) \text{ for each } x \in \Omega, \tag{1}$$

where in EPI $v \in \mathbb{R}^3$ corresponds to the phase-encoding direction. The distortion thus consists of a geometric displacement, limited in direction v, and an intensity modulation ensuring mass-conservation. In other words, due to perturbed field, signal originating from point x is wrongly localized at point $x + \mathcal{B}(x)v$ but the total amount of signal is conserved.

Considering a super-resolution problem, we assume that EPI data are given on a regular coarse grid with N cells of size $\mathbf{H} = [H_1, H_2, H_3]$, and the undistorted image and the unknown inhomogeneity is to be reconstructed on a regular fine grid with n cells of size $\mathbf{h} = [h_1, h_2, h_3]$ and $h_i \leq H_i$ for $i = 1, 2, 3$.

The forward model, that is the simulation of distorted low-resolution EPI data given high-resolution data $I \in \mathbb{R}^n$ and B, is realized using a Particle-In-Cell (PIC) method.[13] PIC methods are widely used in fluid dynamics for solving hyperbolic conservation laws with compressible flows. We place particles in each cell-centres x^j of the fine mesh and attach to them a mass given by the integral of $\mathcal{I}$ over the cell denoted by I^j for $j = 1, \ldots, n$. A continuous image model is then derived from a linear combination of basis functions, where we use linear hat functions centred at the particles' position of width $\epsilon = [\epsilon_1, \epsilon_2, \epsilon_3]$ that are scaled in height such that their integral equals one

$$\mathcal{I}(x) = \sum_{i=1}^{n} I_i\ \Phi_\epsilon(x - x^j),\ \text{where } \Phi_\epsilon(x) = \prod_{d=1}^{3} \frac{1}{\epsilon_d}\phi\left(\frac{x_d}{\epsilon_d}\right) \text{ and } \phi(x) = \begin{cases} 1 - |x| & , x \in [-1, 1] \\ 0 & , \text{else} \end{cases}. \tag{2}$$

Due to the field-inhomogeneity the particles are shifted to the non-grid point $x^i + B^i v$ according to (1). Finally, the image is resampled on the coarse mesh. To this end the mass of the particles is distributed between the adjacent cells of the coarse mesh. The weights are summarized in the *push-forward* matrix

$$T[B, v] \in \mathbb{R}^{N \times n},\ \text{where } (T[B, v])_{i,j} = \int_{\Omega_i^H} \Phi_\epsilon(x - (x^j + B^j v))dx, \tag{3}$$

where Ω_i^H denotes the ith voxel of the coarse mesh. Note that by design of the basis functions each column in T sums to one and thus the total mass is conserved. Overall the forward model summarizes to $I^{\mathrm{EPI}} \approx T[B, v]I$.

Given discrete EPI data $I_1^{\mathrm{EPI}}, \ldots, I_K^{\mathrm{EPI}} \in \mathbb{R}^N$ acquired with phase-encoding directions $v_1, \ldots, v_K$, the inverse problem of estimating the field-inhomogeneity B and the particle weights $I \in \mathbb{R}^n$ on the fine mesh is formulated

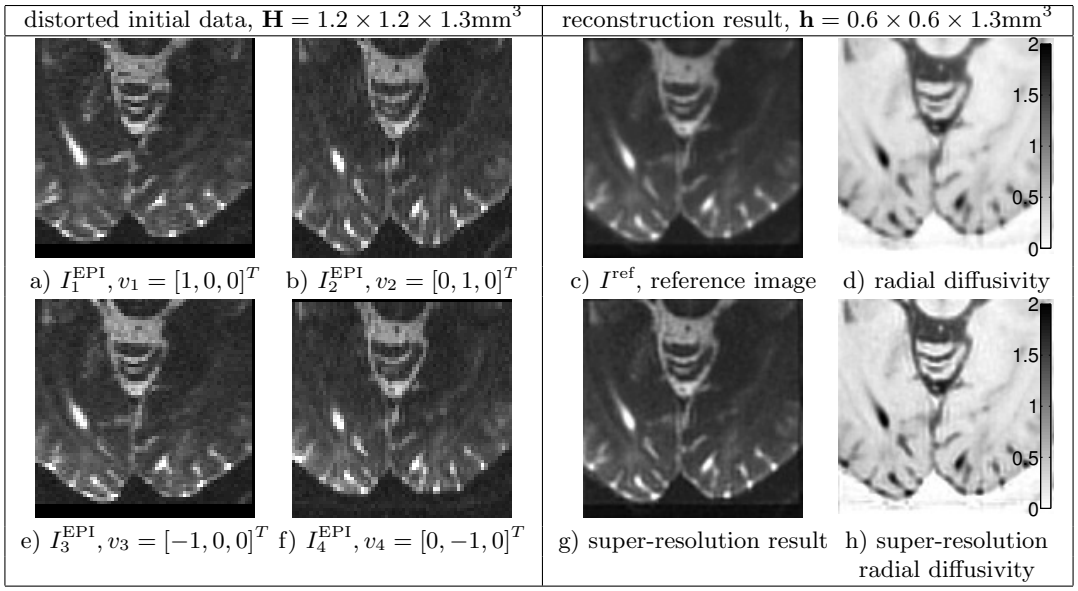

Figure 1. Results of joint 3D super-resolution and susceptibility artefact correction for dMRI data of a human brain. Slice projections of the low-resolution, distorted EPI data with different phase-encoding directions are visualized for one baseline image in a),b),e) and f). Distortion effects are most notable in the posterior region. In c) the reference image, obtained by standard susceptibility artefact correction,[6] averaging and interpolation is shown and in d) the fractional anisotropy (FA) computed from all reference images. The final result of the proposed super-resolution method is visualized in g) and h) by slice projections of the baseline and the radial diffusivity image. To allow comparison, the colormap is identical in all sub-plots. Note that the colormap is inverted in d) and h) to improve visibility.

as a discrete optimization problem

$$J(B,I) = \frac{\text{prod}(\mathbf{H})}{2K} \sum_{k=1}^{K} \left\| T[B,v_k]I - I_k^{\text{EPI}} \right\|^2 + \frac{\text{prod}(\mathbf{h})}{2} (\alpha_1 \|\nabla(B - B^{\text{ref}})\|^2 + \alpha_2 \|\nabla I\|^2 + \alpha_3 \|I - I^{\text{ref}}\|^2) \stackrel{!}{=} \min, \quad (4)$$

where $\alpha \in \mathbb{R}^3$ is a regularization parameter and B^{ref} and I^{ref} are used to incorporate prior knowledge into the optimization. The first term measures the difference between the simulated image and the actual data, while the remaining terms are regularization functionals that ensure smoothness of image and inhomogeneity and deviations from the reference image. For solving (4) we follow the coupled approach outlined in.[8] Noting that for given B the optimality condition for I is linear, we use variable projection, express the high-resolution image in terms of the field-inhomogeneity and solve the reduced minimization problem for B using a standard Gauss-Newton method in MATLAB.

3. RESULTS

A diffusion-tensor dataset of a brain of a healthy volunteer was acquired on a TIM Trio 3T scanner (Siemens Healthcare, Erlangen, Germany). The acquisition protocol provided four dMRI datasets each consisting of measurements along 100 diffusion directions and 11 baseline images without diffusion weighting. For the acquisition of the first two datasets the phase-encoding direction was reversed along the left-right direction yielding an image matrix of 64×128 and 34 slices. For measuring the third and fourth dataset, the phase-encoding direction was reversed along the anterior-posterior axis and the image matrix is 128×64 and 34 slices. For all datasets the voxel size was $1.2 \times 1.2 \times 1.3\text{mm}^3$.

As preprocessing and to provide starting guess and reference models for the optimization problem (4), we corrected each dMRI dataset by using HySCO[6] pair-wise with empirically tuned regularization parameters ($\alpha = 400, \beta = 30$). The estimated inhomogeneity and the initial and corrected image data were cropped to the overlapping domain. Both estimates of the inhomogeneity and the four corrected images were averaged and interpolated to the fine mesh, yielding B^{ref} and I^{ref}, respectively.

The super-resolution images were estimated from (4) using the starting guesses B^{ref} and I^{ref} obtained in the preprocessing step. This procedure was done sequentially for all 100 diffusion weighted image volumes and 11 baseline images with empirically tuned parameter $\alpha = (0.006, 0.1)$ and $\epsilon = [1.5\sqrt{h_1}, 1.5\sqrt{h_2}, h_3/2]$. Figure 1 shows a selected slice of one baseline volume. The coarse initial data, the reference guess and the final result with a voxel-size of $0.6 \times 0.6 \times 1.3\text{mm}^3$ are shown. Finally, diffusion tensors were reconstructed from both the reference images and the results of the proposed super-resolution method. As our method is expected to be most beneficial in the cortex, we visualize radial diffusivity as a marker of neurite microstructure in Figure 1.

4. NEW OR BREAKTHROUGH WORK TO BE PRESENTED

To the best of our knowledge our work combines susceptibility artefact correction and super-resolution in EPI-MRI for the first time. Our method is based on nonlinear deformations and constitutes the first in-plane super-resolution technique in dMRI after Scheffler's critique.[12] Numerical results indicate the unique potential of our technique to provide for the first time in-vivo dMRI at mesoscopic spatial resolution, an essential step towards in-vivo histology.

5. CONCLUSION

In this work we introduce a new method that for the first time allows to jointly correct susceptibility artefacts and increase the in-plane resolution of EPI-MRI. The scheme reconstructs an undistorted, high-resolution image given multiple distorted, low-resolution measurements that are deformed in different directions. In this work, we did not increase the through-slice resolution, however, we note that the phase-encoding direction can be chosen arbitrarily in our setting. Thus, future work will investigate acquisition schemes with phase-encoding gradients in z-direction to provide images of isotropic super-resolution.

REFERENCES

[1] Le Bihan, D., Mangin, J. F., Poupon, C., Clark, C. A., Pappata, S., Molko, N., and Chabriat, H., "Diffusion tensor imaging: concepts and applications," *Journal of Magnetic Resonance Imaging* (2001).

[2] Stehling, M. K., Turner, R., and Mansfield, P., "Echo-planar imaging: magnetic resonance imaging in a fraction of a second," *Science* (1991).

[3] Jezzard, P. and Balaban, R. S., "Correction for geometric distortion in echo planar images from B0 field variations," *Magnetic Resonance in Medicine* (1995).

[4] Ruthotto, L., Kugel, H., Olesch, J., Fischer, B., Modersitzki, J., Burger, M., and Wolters, C. H., "Diffeomorphic Susceptibility Artefact Correction of Diffusion-Weighted Magnetic Resonance Images," *Physics in Medicine and Biology* (2012).

[5] Chang, H. and Fitzpatrick, J. M., "A technique for accurate magnetic resonance imaging in the presence of field inhomogeneities," *IEEE Transactions on Medical Imaging* (1992).

[6] Ruthotto, L., Mohammadi, S., Heck, C., Modersitzki, J., and Weiskopf, N., "HySCO - Hyperelastic Susceptibility Artifact Correction of DTI in SPM," in [*Bildverarbeitung für die Medizin 2013*], (2013).

[7] Heidemann, R. M., Anwander, A., Feiweier, T., Knösche, T. R., and Turner, R., "k-space and q-space: Combining ultra-high spatial and angular resolution in diffusion imaging using ZOOPPA at 7T," *NeuroImage* (2012).

[8] Chung, J., Haber, E., and Nagy, J., "Numerical methods for coupled super-resolution," *Inverse Problems* (2006).

[9] Greenspan, H., Oz, G., Kiryati, N., and Peled, S., "MRI inter-slice reconstruction using super-resolution," *Magnetic Resonance Imaging* (2002).

[10] Mai, Z., Verhoye, M., Van der Linden, A., and Sijbers, J., "Diffusion tensor image up-sampling: a registration-based approach," *Magnetic Resonance Imaging* (2010).

[11] Poot, D. H., Jeurissen, B., Bastiaensen, Y., Veraart, J., Van Hecke, W., Parizel, P. M., and Sijbers, J., "Superresolution for multislice diffusion tensor imaging," *Magnetic Resonance in Medicine* (2013).

[12] Scheffler, K., "Superresolution in MRI?," *Magnetic Resonance in Medicine* (2002).

[13] Grigoryev, Y. N., Vshivkov, V. A., and Fedoruk, M. P., [*Numerical "Particle-in-Cell" Methods: Theory and Applications*], De Gruyter (2002).